Paper: ASAT-16-059-EP

16th International Conference on
AEROSPACE SCIENCES & AVIATION TECHNOLOGY,
ASAT - 16 – May 26 - 28, 2015, E-Mail: asat@mtc.edu.eg
Military Technical College, Kobry Elkobbah, Cairo, Egypt
Tel : +(202) 24025292 – 24036138, Fax: +(202) 22621908

Hybrid Fuel Cell – Battery Powered System for Long Duration Flight

Karim N. Mobariz[1], Ahmed M. Youssef [2+], Mohamed A.L. Badr[3], Mohamed Abdel-Rahman[4]
[1] Ph.D. Candidate, Egyptian Armed Forces, Egypt
[2] Associated Professor, Egyptian Armed Forces, Egypt
[3] Professor, Electrical Power Engineering, Ain Shams University, Egypt
[4] Associated Professor, Electrical Power Engineering, Ain Shams University, Egypt

Abstract. Unmanned aerial vehicles (UAVs) have received considerable attention in many civilian and military fields. Performing environmental monitoring, and surveying applications have very specific constraints on power, cost, weight, and flight endurance. Because of the limited flight duration of electric UAVs that are powered by only batteries, this paper proposed the development of a new power system for long endurance UAVs propulsion application. This power system consists of a fuel cell stack, a pack of Lithium-ion batteries, and a DC-DC buck converter.

Normally, using Jacobian linearization via a Taylor series expansion at the nominal operating point cannot achieve satisfactory dynamic performance under sudden changes in the loads. Therefore, nonlinear dynamic models of both the fuel cell and the Lithium-ion battery are developed. The structure of buck converter is also studied and its different parts are introduced. A buck converter optimized PID controller is designed to convert the stack voltage into standard DC and to achieve a satisfactory transient behavior. This PID controller is tuned by the gradient descend multi-parameter-optimization technique. The proposed system is modeled and simulated using MATLAB/Simulink software. Simulation results showed that a hybrid combination of hydrogen fuel cells and Lithium-ion batteries can fulfill the requirements of a long endurance UAV power source and verified the capability of the designed system to maintain the output voltage constant under sudden changes in the loads.

1. Introduction

Unmanned aerial vehicles (UAVs) have received considerable attention in many military and in law enforcement missions (e.g., reconnaissance, remote delivery of urgent equipment/material, battlefield monitoring, etc). UAVs have also gained popularity in civilian applications (geological surveying, search and rescue operations, etc). The reason for this attention is that UAV platforms are low-cost and viable alternatives to manned aircraft as valuable sources of data for much application. For UAVs to perform these long endurance applications, their power sources need to be developed to ensure the long endurance functionality of the propulsion system and onboard equipment [1].

+ Corresponding author. Tel.: +202-2401-9428.
E-mail address: ammyk_khater@yahoo.com.

Although long endurance is achievable with conventional fuels, hydrocarbon-fueled systems are usually loud, inefficient, and unreliable when it comes to those small flying vehicles. On the other hand, batteries do not offer enough power for battery-powered systems for a long duration flight due to the low energy density of the battery system, especially where cameras and other equipment – powered by the same battery as the UAV's propulsive system – are in use. In addition to that, the longer battery charging time is another constraint to limit the pure battery driven vehicles. Therefore researchers started the development of powering long endurance UAVs by renewable and clean energy sources. Alternatives to the combustion of gasoline and other fossil fuels, renewable energy sources offer higher power and energy densities, lower cost, non-carbon emission, more-efficient power, lower acoustic and heat emissions which are also required to hinder detection and facilitate performing the missions. One of these renewable energy sources of electric power is the fuel cell.

A fuel cell is an electro-chemical device that converts chemical energy into electrical energy and heat as a byproduct. The fuel cell will continuously deliver electric power as long as fuel is supplied. The most commonly used fuels are hydrogen and oxygen. There are many types of fuel cells available today: such as proton exchange membrane fuel cells, alkaline fuel cells, phosphoric acid fuel cells, solid oxide fuel cells, and molten carbonate fuel cells [2,3]. In this paper, Polymer Electrolyte Membrane or Proton Exchange Membrane fuel cells (PEMFCs) are used because of their comparatively high efficiency, high energy density, low working temperature ($30-100^{o}C$), compactness, easy and safe operational modes, in addition of being available in the marketplace for a variety of different systems [4, 5].

Unfortunately fuel cells have some disadvantages such as slow dynamic response time, relatively long warming up time before full power output is available, and their stack output voltage are sensitive to sudden changes in the loads [2]. On the other hand, the battery has a fast dynamic response time to fluctuations in a load, and has high power density therefore; the hybrid solution between the PEMFCs and Lithium-ion batteries represents one of the ideal power solutions for long endurance UAV flights. This hybrid system allows exploitation of the advantages of both energy sources and undermines their disadvantages. A DC–DC buck converter is proposed to step-down the fuel cell stacks output voltage to a desired value. Hence, a fuel cell stack, a pack of Lithium-ion batteries, and a DC-DC buck converter will constitute the fuel cell-battery hybrid system.

A PID controller is suggested for the DC–DC buck converter to ensure a constant output voltage and to reject the disturbance from load and fuel cells stacks. Traditionally, ad-hoc methods have been used to choose PID parameters. In this work, multi-parameter optimization technique is used for tuning the gains of the PID controller. This decreases the time and effort for tuning parameters considerably and proves that the day of ad-hoc methods for tuning PID controllers is ending [6].

The paper is organized in six sections: Section 2 describes briefly the components of the fuel cell-battery hybrid system. Section 3 details the operational characteristics and the mathematical modeling of the PEMFC, the Lithium-ion battery, and the DC-DC buck converter. In Section 4, the whole system is implemented in the Simulink environment, and a description of the UAV's mission scenario is presented. The design of the buck converter controller is detailed and the simulation results are explained in Section 5. Finally, the paper concludes with a brief summary in Section 6.

2. Hybrid System Description

Fig. 1 shows the proposed fuel cell-battery hybrid power system. It consists of a PEMFC as a primary power source and a pack of Lithium-ion batteries as a second power source. A DC-DC buck converter is used to step down the voltage to power: (i) a continuous load; a BLDC motor which represents the propulsive electric motor and (ii) suddenly changing loads; such as camera and servos.

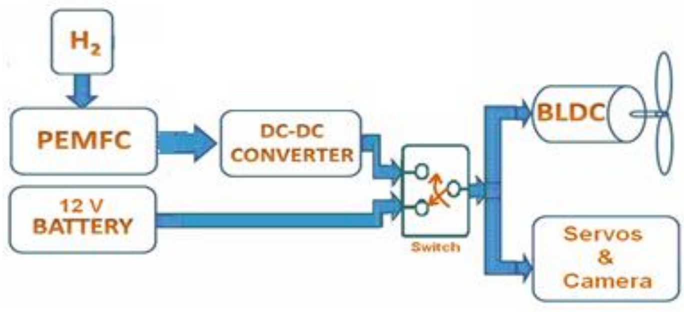

Fig. 1: Hybrid fuel cell-battery hybrid power system

3. System Modelling

3.1. Polymer electrolyte \ proton exchange membrane fuel cell

A PEMFC consists of a solid polymer electrolyte membrane sandwiched between two electrodes (anode and cathode), as shown in Fig. 2. When the hydrogen is injected at the anode and enters the electrolyte, it ionizes [2, 7].

Anode: $H_2 \rightarrow 2H^+ + 2e^-$ (1)

Only protons are allowed to pass through the electrolyte, therefore the protons move across the electrolyte to the cathode to rejoin with oxygen, while the freed electrons from the hydrogen atoms travel through an external circuit to recombine with oxygen at the cathode.

Cathode: $O_2 + 4H^+ + 4e^- \rightarrow 2H_2O$ (2)

Therefore, the overall chemical reaction becomes:

$2H_2 + O_2 \rightarrow 2H_2O +$ Electricity + heat (3)

i.e., hydrogen gas is recombined with oxygen gas producing electricity with water vapor as emission. A closed loop system could be operated whereby the water from of the PEMFC can be electrolyzed into oxygen and hydrogen for later re-use. Oxygen is generally obtained from the surrounding air.

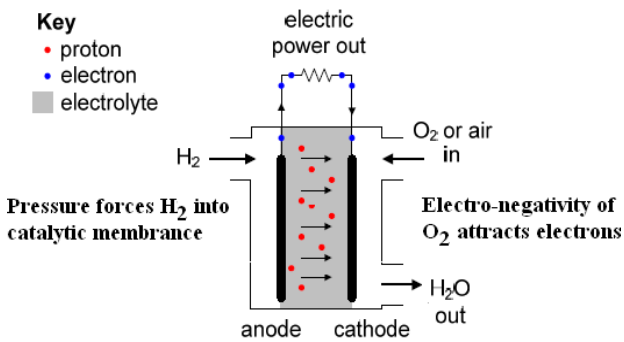

Fig. 2: Single PEMFC

Typically, a single fuel cell produces voltage between 0 and 1V. The relationship between output voltage and load current is given as:

$$V = E - \underbrace{(i+i_n)r}_{\text{Ohmic loss}} - \underbrace{A\ln\left(\frac{i+i_n}{i_0}\right)}_{\text{Activation loss}} + \underbrace{B\ln\left(1-\frac{i+i_n}{i_l}\right)}_{\text{Concentraion loss}} \quad (4)$$

To produce a higher voltage, multiple cells have to be connected in series to build a fuel cell stack. Fig. 3 shows our fuel cell stack, which comprises 14 cells; the parameters of each are listed in Table 1.

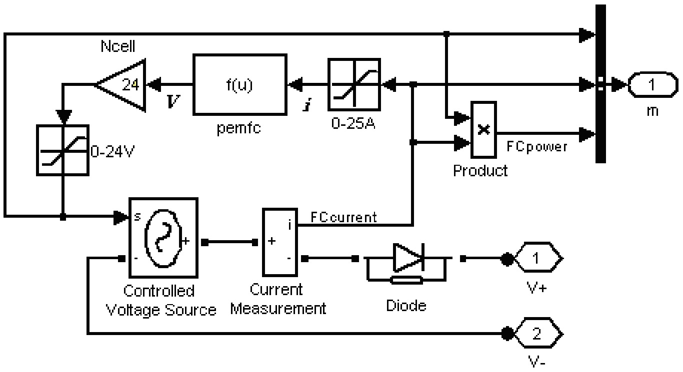

Fig. 3: Simulink model of PEMFC stack

Table 1: Single PEMFC parameters

Parameter	Value
Open circuit voltage *E*	1.2 volt
Internal current density i_n	2 mA/ cm^2
Internal resistance *r*	0.00003 kΩ.cm^2
Activation losses constant *A*	0.06 volt
Exchange current density i_0	0.067 mA/ cm^2
Concentration losses constant *B*	0.05 volt
Limit current density i_l	900 mA/ cm^2

3.2. Lithium-ion Battery

Lithium-ion battery is chosen to be the second energy source with the PEMFC in the hybrid system because of its relatively high specific power and energy, high energy efficiency and long cycle life [8]. Lithium-ion battery model is introduced in Fig. 4. The parameters of used battery (model no.:BP2546) are shown in Table 3 [9].

Table 3: Parameters of Lithium-ion battery

Parameter	Value
Nominal Voltage	3.7V
Rated Capacity	3350mAh
Charge Voltage	4.2V

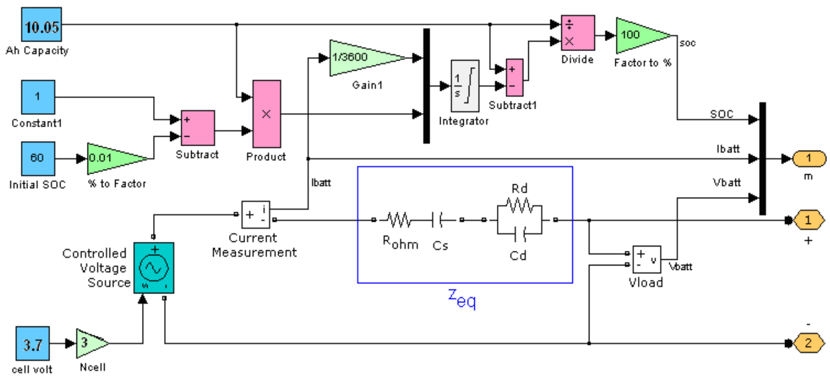

Fig. 4: Lithium-ion battery model

3.3. Buck Converter

Buck converter is a type of switching-mode power supply which is used for stepping-down DC voltage level. It uses two switches (a MOSFET and a diode), an inductor and a capacitor. In Fig 5, when a positive signal is applied at the MOSFET gate (g > 0), the DC input voltage V_{in} from the PEMFC is allowed to charge the inductor and to supply output voltage V_{out} across the output capacitor

C_{out}. Charging will continue till V_{out} reaches to reference voltage V_{ref}, then the control part turns OFF the switch (g = 0). The inductor will then change its voltage polarity and the current will flow in the same direction through the diode which is turned ON by switch controller part. Discharging will continue until V_{out} reaches below V_{ref}, then control part again turns ON the MOSFET to compensate V_{out} drop and this cycle continues until complete regulation of V_{out} [10]. This process is accomplished by sensing the output voltage of the circuit by means of a negative feedback loop to the pulse-width-modulation (PWM) generator which controls the ON and OFF states of the MOSFET switches.

Controlling the switches, or in other words changing the duty cycle *D* to keep V_{out} equal to V_{ref} can be explained as follows: the error voltage ($V_E = V_{ref} - V_{out}$) is compared to sawtooth ramp V_{saw} generated by ramp generator, if voltage V_E is higher than V_{saw} as in Fig. 6, the PWM generator reduces the duty cycle by holding ON the MOSFET gate for a short time of every cycle. While V_E is lower than V_{saw}, the PWM generator increases the duty cycle by holding ON the gate for the most of cycle to rectify the output voltage.

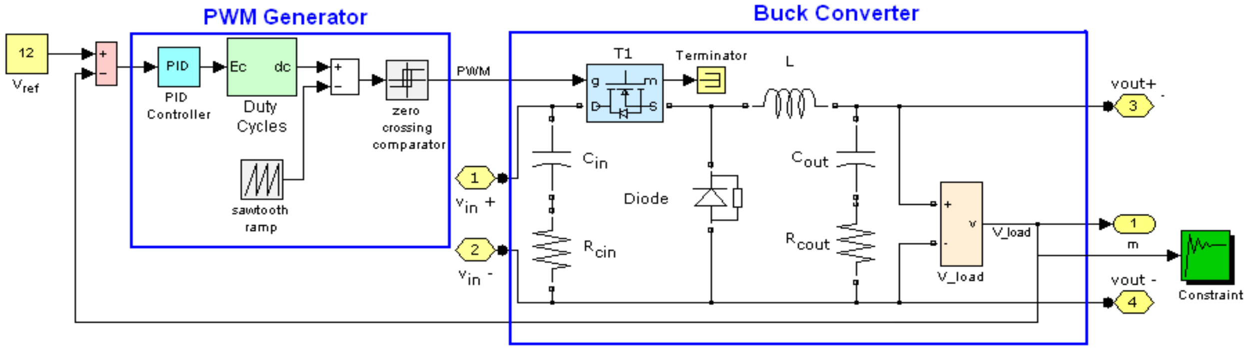

Fig. 5: Buck converter control loop

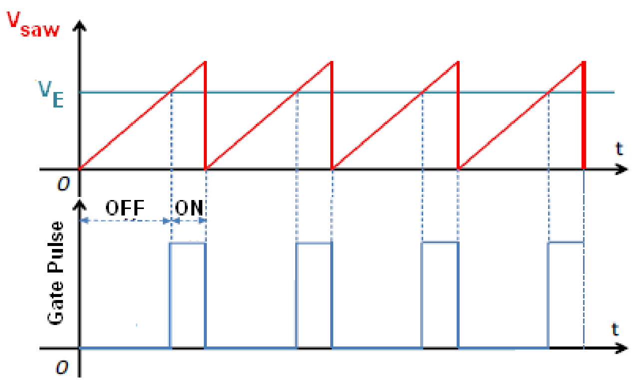

Fig. 6: PWM controlled input voltage

The duty cycle is the ratio of the output voltage to the input voltage considering the voltage applied on diode V_F and MOSFET V_{out} as shown in Eq.(5), and it has a value in the interval 0 to 1.

$$D = \frac{V_{out} + V_F}{V_{in} - V_{RDSon}} \qquad (5)$$

The selection criterion of the buck converter elements is explained as follows: the output capacitor (C_{out}) is chosen to filter the switching ripple; its capacitance must be large enough so that its impedance is much smaller than the load at the switching frequency, allowing most of the ripple current to flow through the capacitor, not the load. The output capacitor's equivalent series resistance R_{Cout} must also be taken into account because its parasitic resistance causes additional voltage ripple [11]. The output voltage ripple V_{ripple} and the minimum output current I_{min} are assumed to be 1% of V_{out} and 10% of I_{out}, respectively:

$$C_{out} \geq C_{out\,\min} \qquad C_{out\,\min} = \frac{2 * I_{\min} * T}{8 * V_{ripple}} \tag{6}$$

The input capacitor (C_{in}) deals with highest ripple current. An acceptable level of the input voltage ripple $V_{rippleIN}$ is assumed to be 5% of V_{in}.

$$C_{in} \geq C_{in\,\min} \qquad C_{in\,\min} = \frac{I_{peak} * T}{8 * V_{rippleIN}} = \frac{I_{peak} * T}{8 * (0.05 * V_{in})} \tag{7}$$

The minimum inductor value (L_{min}) is calculated as follows:

$$L \geq L_{\min} \qquad L_{\min} = \frac{(V_{in} - V_{out} - V_{RDSon}) * T_{on}}{2 * I_{\min}} \tag{8}$$

According to the above equations, the calculated buck converter parameters are listed in Table 4.

Table 4: Buck converter parameters

Parameter	Symbol	Value	Unit	Parameter	Symbol	Value	Unit
Output voltage of converter	V_{out}	12	V	Duty cycle	D	0.888	
Input voltage of converter	V_{in}	14	V	Switching period	T	20	μ sec
Nominal output current	I_{out}	2	A	On-time of the switch	T_{on}	17.754	μ sec
Peak switching current	I_{peak}	2.2	A	Inductor value used	L	5665	μH
Maximum allowable peak-to-peak ripple	V_{ripple}	0.12	V	Output bank capacitance	C_{out}	220	μF
Drain to source resistance at switching on	R_{DSon}	0.1	Ω	Internal resistance of (C_{out}) used	R_{Cout}	0.015	Ω
Forward voltage drop across diode	V_F	0.25	V	Capacitance of input bank	C_{in}	500	μF
Voltage drop across R_{DSon}	V_{RDSon}	0.2	V	Internal resistance of (C_{in}) used	R_{Cin}	0.1	Ω

4. System Integration and Mission Scenario

The sub-systems are integrated in the Simulink environment as shown in Fig.7. The scenario of UAV's mission is shown in Fig. 8. At start-up process, the Lithium-ion battery is used to supply the power to the propulsive BLDC motor due to its fast dynamic response time of milliseconds. Then after 30 sec, the hydrogen fuel pump is switched ON to supply the fuel to the fuel cells, which in turn take about 30 seconds for the fuel cell reactions and the stack heating to reach power at maximum efficiency and hence the battery is switched OFF.

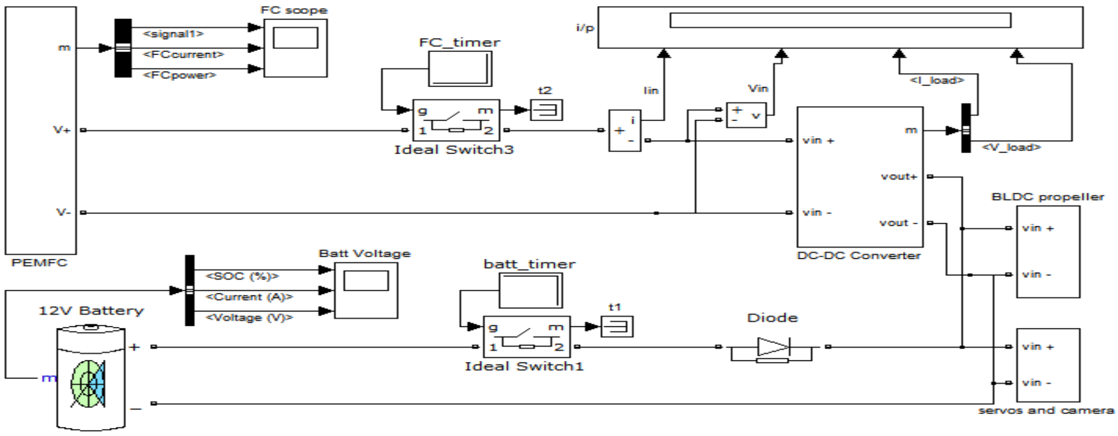

Fig. 7: Hybrid system Simulink model

The UAV's mission begins with the take-off and climbing modes; using the elevator control surface, and lasts until the desired altitude is achieved. Then the UAV starts to fly horizontally towards the target destination. After flying 20 min, the camera is switched ON for about 45 min. After finishing its mission, the UAV returns back to reach the landing site again using both the ailerons and rudder control surfaces, followed by descending mode using the elevator control surface.

Table 5: Scenario of UAV's mission

Process	**Time interval [min]**	**Description**	**Source**	**Loads**
1	0 – 1	Engine Start-up (Battery ON)	Battery	BLDC 13Ω
2	1 – 2	Taxing & Taking Off (Battery OFF)	Fuel cell via buck	BLDC 13Ω
3	2 – 10	Climbing		BLDC 13Ω + elevator 30Ω
4	10 – 20	Horizontal flight		BLDC 13Ω
5	20 – 65	Camera ON		BLDC 13Ω+camera 14Ω
6	65 - 66	Camera OFF Turning		BLDC13Ω + ailerons30Ω + rudder30Ω
7	66 - 110	Return - Horizontal flight		BLDC 13Ω
8	110 - 118	Descending		BLDC 13Ω + elevator 30Ω
9	118 – 120	Landing & Taxing		BLDC 13Ω
10	120	Engine Shut-down		-----

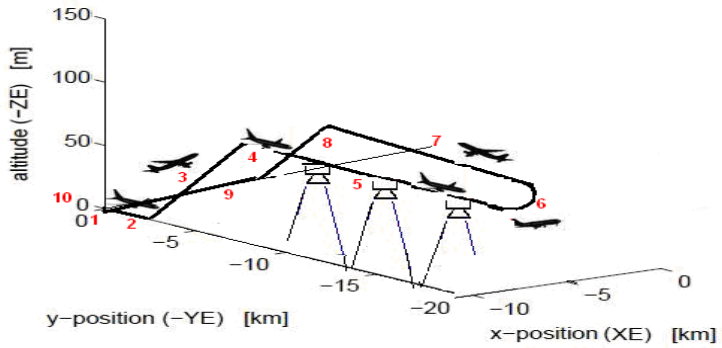

Fig. 8: UAV mission scenario

The amounts of power consumed by the loads vary according to their resistant loads. Table 5 summarizes the scenario of UAV's mission and illustrates the resistant loads of the propulsive BLDC motor [12], the control surfaces actuators and the camera.

5. Buck Converter Controller Design and Simulation Results

Although a PID controller is one of the earlier control strategies, it still has a wide range of applications in industrial control due to its easily implementation in the field environment.

A mathematical description of the PID controller is:

$$u(t) = K_p e(t) + K_i \int_0^t e(\tau)\, d\tau + K_d \frac{d\,e(t)}{dt} \tag{9}$$

where in our case; Fig. 5, $u(t)$ is the input signal to the duty cycles block, the error signal $e(t)$ is defined as $e(t) = V_{ref} - V\_load$. K_p, K_i, and K_d are the proportional, integral, and derivative gains, respectively.

Unlike traditional trial-and-error methods for obtaining PID gains, gradient descent optimization method is used to adjust these gains within a nonlinear Simulink model to meet time-domain performance requirements by graphically placing constraints within a time-domain window and closely matching a reference signal.

After few iterations, the optimal and feasible PID gains obtained were 8, 30, and 0.009 related to K_p, K_i and K_d, respectively. The simulation results for the whole hybrid system; Fig. 7, are given in Figs. 9-12.

As shown in Fig. 9, BLDC motor is started-up using the battery only, where the PEMFC gives no output current. One minute later, the fuel cell became capable of feeding the whole system thus the battery is disconnected. During horizontal flight as shown in Figs. 11 and 12, the BLDC motor; the only load, is powered via the buck converter, the load output current drawn is 0.92A and the output voltage is 12V.

It was clear from Fig. 10 and Fig. 12, that the fuel cell stack output voltage is sensitive to sudden changes in the loads, and that the designed optimized PID controller is capable to convert the stack voltage into standard DC and to achieve a satisfactory transient behavior.

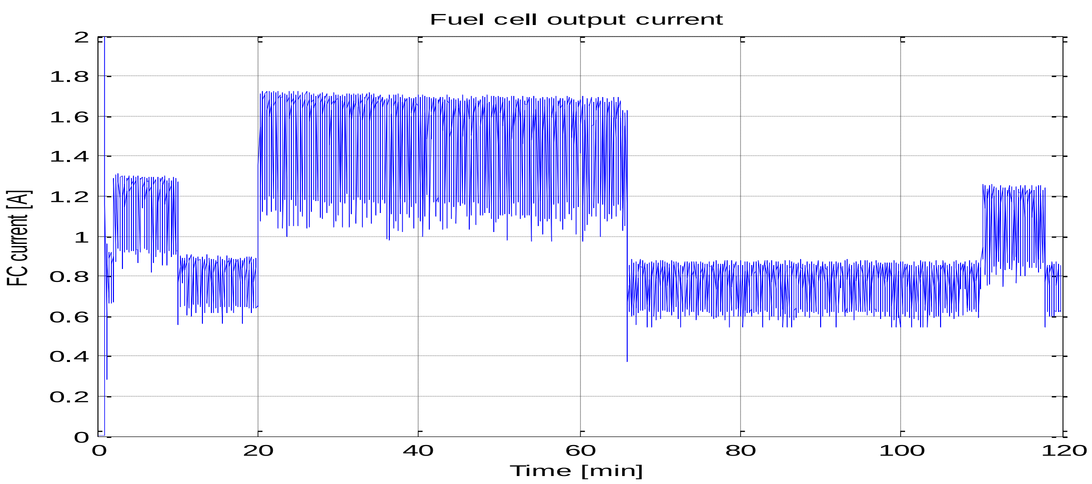

Fig. 9: Fuel cell output current

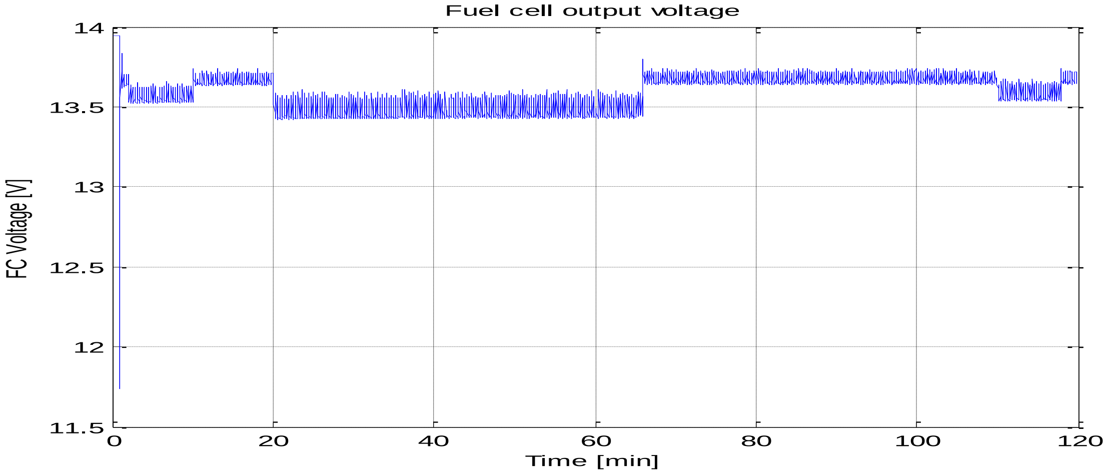

Fig. 10: Fuel cell output voltage

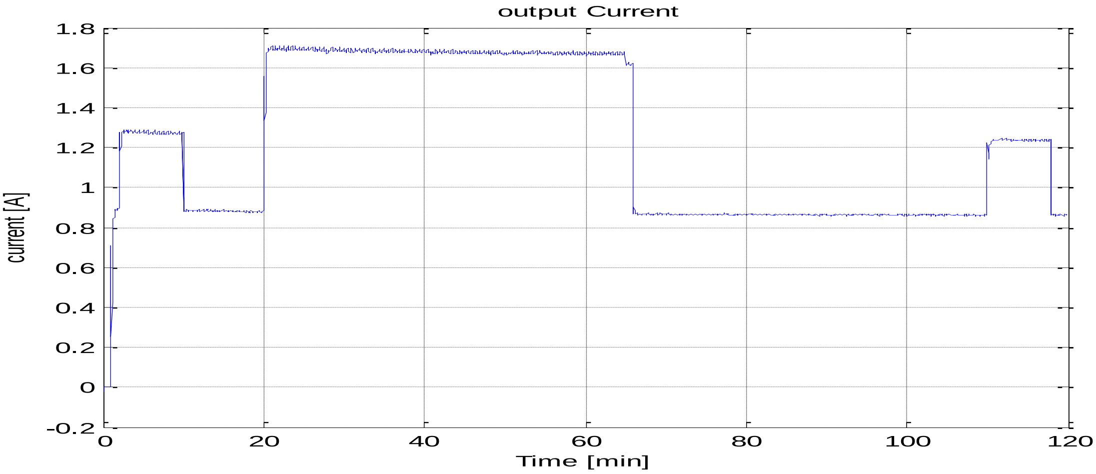

Fig. 11: Converter Output current

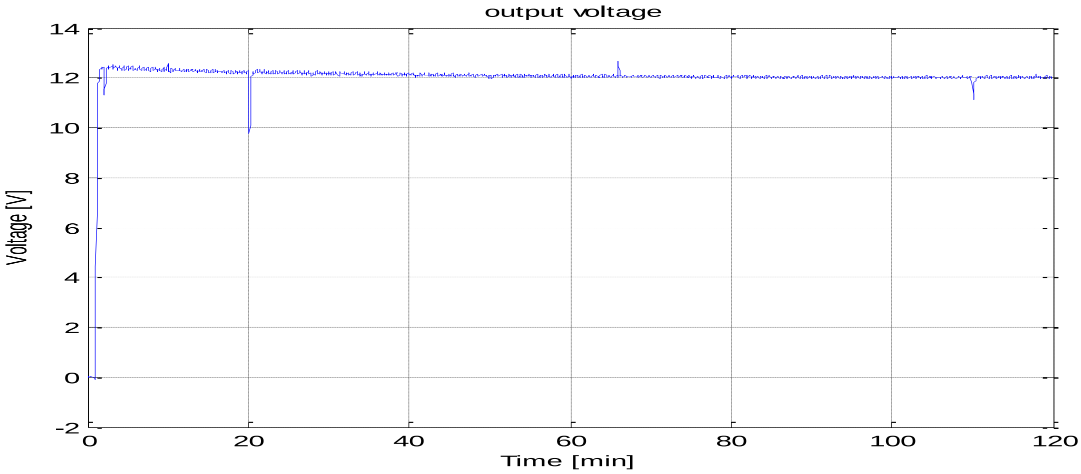

Fig. 12: Converter Output voltage

6. Conclusions

Because of the limited flight endurance of electric UAVs that are powered by only batteries, this paper proposed a new power system for long endurance flight applications. This power system consists of a fuel cell stack, a pack of Lithium-ion batteries, and a DC-DC buck converter.

Detailed description for fuel cell and Lithium-ion battery models is involved. Building the DC-DC buck converter and selecting criterion of its elements were also explained. Designing an optimal PID controller; for the buck converter, using the gradient descend multi-parameter-optimization technique is presented. The proposed system is modeled and simulated using MATLAB/Simulink environment. Simulation results verified the capability of the designed system to maintain the output voltage constant under sudden changes in the loads.

References

[1] J. Meyer, F. du Plessis, and et al. *Aerial Vehicles: Design considerations for long endurance unmanned aerial vehicles*. Intech, Chapter 22, 2009.

[2] R. Smith. *Design of a control strategy for a fuel cell-battery hybrid power supply*. M.Sc. dissertation, Texas A & M University, USA, 2009.

[3] EG&G Services, Inc. *Fuel Cell Handbook*. Science Applications International Corporation, 2004 (Seventh Edition).

[4] M. Dudek, P. Tomczyk, and et al. Hybrid fuel cell - battery system as main power unit. *International Journal of Electrochemical Science*, 2013, 8: 8442-8463

[5] L. Karunarathne. *An Intelligent Power Management System for Unmanned Aerial Vehicle Propulsion Applications*. Ph.D. dissertation, Cranfield University, UK, 2012.

[6] A. Youssef. Optimized PID tracking controller for piezoelectric hysteretic actuator model. *World Journal of Modelling and Simulation*, 2013, 9:223-234.

[7] J. Han, J. Charpentier, and et al. *An Energy Management System of a Fuel Cell/Battery Hybrid Boat*. Energies, 2014, 7: 2799-2820.

[8] S. Mantravadi. *Modeling, simulation and implementation of Li-ion battery powered electric and plug-in hybrid vehicles*. M.Sc. dissertation, University of Akron, USA, 2011.

[9] Electronic Components Datasheets Search. *Panasonic Battery Group*. http://www.alldatasheet.com/datasheet-pdf/pdf/597043/PANASONICBATTERY/NCR18650B.html

[10] N. Safari. *Design of a DC/DC buck converter for ultra-low power applications in 65nm CMOS Process*. M.Sc. dissertation, Linköping University, Sweden, 2012.

[11] Buck calculator. *Texas Instruments*. http://focus.ti.com/download/aap/utilities/buck.xls

[12] Moog Components Group, *Miniature Brushless DC Motors: DBH-0472 motor Datasheet*, August 2006.